Activation of FOXO3a by the Green Tea Polyphenol Epigallocatechin-3-Gallate Induces Estrogen Receptor α Expression Reversing Invasive Phenotype of Breast Cancer Cells

Karine Belguise, Shangqin Guo, and Gail E. Sonenshein

Department of Biochemistry and Women's Health Interdisciplinary Research Center, Boston University School of Medicine, Boston, Massachusetts

Abstract

Previously, we showed that the bioactive green tea polyphenol epigallocatechin-3-gallate (EGCG) inhibits growth in soft agar of breast cancer cells with Her-2/neu overexpression. Using gene expression profiling, here we show that EGCG treatment of Her-2/neu–driven mammary tumor cells alters the expression of key regulators in the epithelial to mesenchymal transition (EMT) pathway, reducing invasive phenotype. Specifically, the epithelial genes *E-cadherin, γ-catenin, MTA3*, and *estrogen receptor α* (*ERα*) were up-regulated by EGCG, whereas the proinvasive *snail* gene was down-regulated. Consistently, EGCG inhibited branching colony growth and invasion in Matrigel. EGCG treatment similarly inhibited invasive phenotype of mouse mammary tumor cells driven by Nuclear Factor-κB c-Rel and protein kinase CK2, frequently found overexpressed in human breast disease. Recently, we identified the Forkhead box O transcription factor FOXO3a as a major transcriptional regulator of ERα. Given the pivotal role of ERα in preventing EMT, we hypothesized that the activation of FOXO3a by EGCG plays an important role in the observed reversal of invasive phenotype in ERα-positive breast cancer cells. EGCG treatment activated FOXO3a. Ectopic expression of a constitutively active FOXO3a overrode transforming growth factor-β1–mediated invasive phenotype and induced a more epithelial phenotype, which was dependent on ERα expression and signaling. Conversely, a dominant negative FOXO3a reduced epithelial phenotype of ERα-low breast cancer cells. These results identify, for the first time, a role for FOXO3a in the inhibition of invasive phenotype in breast cancer cells with active ERα signaling and elucidate a novel mechanism whereby EGCG represses EMT of breast cancer cells. [Cancer Res 2007;67(12):5763–70]

Introduction

Consumption of tea around the world is believed second only to water, although the levels vary widely by country. Green tea is rich in polyphenols, which have potent antioxidant properties. The most abundant polyphenol in green tea is epigallocatechin-3 gallate (EGCG). Many cancer epidemiologic studies have shown an inverse association between green tea consumption and cancer incidence, of which breast cancer risk reduction and tea consumption are among the best characterized (1). For example, consumption of green tea was closely associated with decreased numbers of axillary lymph node metastases among premenopausal patients with stage I and II breast cancer and with increased expression of progesterone receptor and estrogen receptor α (ERα) among postmenopausal women (2). An inverse correlation between regular green tea consumption before breast cancer diagnosis and the subsequent risk of recurrence has also been shown (3).

Studies using animal models have similarly shown a powerful protective role of green tea against mammary gland malignancies. Initial studies were done with chemical carcinogens. For example, diets containing green tea catechins significantly increased survival of female Sprague-Dawley (S-D) rats treated with 7,12-dimethylbenz(a)anthracene (DMBA) compared with those given regular chow diet (4). In work from our group, S-D rats were given either 0.3% green tea or water as their sole fluid source and then treated with DMBA. We observed a significant increase in mean latency to first tumor, an approximate 70% decrease in tumor burden, and an 87% reduction in the number of invasive tumors per tumor-bearing animal in the rat group drinking green tea (5). Similar protection has been seen in other animal models of cancer, including those of the prostate, skin, and lung (1). For example, oral infusion of a polyphenolic fraction isolated from green tea significantly inhibited prostate cancer development and increased survival in the transgenic adenocarcinoma of mouse prostate (TRAMP) mouse model (6). Furthermore, oral application of green tea polyphenols resulted in markedly reduced tumor size in UV B–induced DMBA-initiated skin tumors in mice (7).

To begin to examine the molecular mechanisms of green tea action, we have turned to cells in culture transformed by specific oncogenes, e.g., Her-2/neu or ErbB2, the second member of the epidermal growth factor (EGF) receptor family or the Nuclear Factor-κB (NF-κB) c-Rel subunit. Her-2/neu is overexpressed in about 30% of human breast cancers and indicates poor prognosis. Her-2/neu overexpression confers anchorage-independent growth and invasion properties *in vitro* (8), and correlates with axillary lymph node positivity and the presence of vascular invasion and metastases in breast cancer patients (9). The gene expression signature of Her-2/neu–transformed tumor cells shows high expression of genes promoting proliferation, migration, invasion, and metastasis and low expression of those promoting apoptosis and immune response (10). Constitutive activation of the phosphoinositide-3-kinase (PI3K) to Akt/protein kinase B to NF-κB signaling pathway has been implicated in the induction of growth and transformed phenotype of Her-2/neu–overexpressing cells (11–13). Of note, we observed that treatment of Her-2/neu–overexpressing breast cancer cells with EGCG reduced PI3K, Akt, and NF-κB activity and anchorage-independent growth (14).

Epithelial to mesenchymal transition (EMT), which has been recognized for several decades as a critical feature of embryogenesis,

Note: K. Belguise and S. Guo contributed equally to the studies.

Requests for reprints: Gail E. Sonenshein, Department of Biochemistry, Boston University School of Medicine, 715 Albany Street, Boston, MA 02118. Phone: 617-638-4120; Fax: 617-638-4252; E-mail: gsonensh@bu.edu.

©2007 American Association for Cancer Research.

doi:10.1158/0008-5472.CAN-06-4327

Downloaded from http://aacrjournals.org/cancerres/article-pdf/67/12/5763/2569018/5763.pdf by guest on 04 May 2023

has more recently been shown to be relevant for cancer. During EMT, cancer cells lose expression of proteins that promote cell-cell contact such as E-cadherin and γ-catenin and acquire mesenchymal markers such as the zinc-finger transcription factor Snail, vimentin, fibronectin, and N-cadherin (15, 16), which promote cell migration and invasion (17). Recent work by several groups has uncovered a signaling pathway that inhibits EMT in cancer cells linked to ERα signaling. Transcription of MTA3, a component of the histone deacetylase NuRD, is regulated by ERα (16). In turn, NuRD represses transcription of the gene encoding Snail, which represses E-cadherin gene transcription (18). Thus, ERα plays a central role in the control of EMT. The expression status of Her-2/neu and ERα correlate inversely in breast cancer (19, 20). Reduced ERα activity in breast tumors is frequently associated with a switch from an epithelial architecture to induction of invasive growth (15, 16). We recently showed that ERα synthesis is controlled by the Forkhead family transcription factor FOXO3a, and that the activity of FOXO3a is greatly reduced in Her-2/neu–driven cancers due to constitutive Akt kinase activity (21). Because Her-2/neu–mediated activation of Akt was repressed upon EGCG treatment (14), here we tested the hypothesis that activation of FOXO3a by EGCG can revert invasive phenotype of breast cancer cells that are ERα low. We show that EGCG represses invasive phenotype of breast cancer cells driven by Her-2/neu, as well by the NF-κB c-Rel subunit and protein kinase CK2, via inducing FOXO3a, which activates the ERα to E-cadherin pathway leading to an epithelial expression profile. Thus, our studies elucidate, for the first time, a novel functional role of FOXO3a as an important upstream mediator of the anti-invasive effects of ERα in breast cancer cells.

Materials and Methods

Cell growth and treatment conditions. The mouse mammary tumor virus (MMTV)–Her-2/neu cell line NF639 (kindly provided by P. Leder, Harvard Medical School, Boston, MA) was derived from a mammary gland tumor and cultured as described previously (22). The rel-3875 line was derived from a mammary adenocarcinoma with poorly differentiated large cells that developed in the MMTV–c-*rel* mouse (23). The rel/CK2-5839 cell line was derived from a mammary adenocarcinoma in the MMTV–c-*rel* × MMTV-CK2α bitransgenic mouse (24). The NF639, rel-3875, and rel/CK2-5839 cells are invasive and express low levels of ERα (ref. 21 and see below). NMuMG, which is an untransformed, immortalized mouse mammary epithelial cell line, was cultured as described previously (25). The MDA-MB-231 ERα-negative breast cancer cell line was grown as described previously (24). EGCG, purchased from LKT Laboratories Inc., was dissolved in sterile DMSO. ICI 182,780 and transforming growth factor-β1 (TGF-β1) were purchased from Tocris Cookson and R&D Systems, respectively.

Plasmid constructs and transfection analysis. The expression vectors for wild-type (WT) FOXO3a, constitutively active A3 FOXO3a mutant, dominant negative FOXO3a (FOXO DN), and parental pECE vectors were kindly provided by M. Greenberg and A. Brunet (Harvard Medical School, Boston, MA; ref. 26). In the A3 mutant, three sites of Akt phosphorylation of FOXO3a (T32, S253, S315) were mutated to alanine residues. The dominant negative TM ΔDB FOXO3a mutant has a deletion in the DNA binding domain and no longer binds to DNA; however, it still localizes in the nucleus and may titer transcriptional coactivators away from endogenous FOXO, thereby exerting a dominant-negative effect (27). The *E-cadherin* promoter reporter vector contained −21 bp of the *E-cadherin* gene (28) subcloned into the pGL3-Basic luciferase (Luc) reporter construct. The SV40 β-galactosidase (β-gal) reporter vector (23) was used to normalize transfection efficiency. For reporter assays, cells were plated in 6- or 12-well plates, and 24 h later, cells were transfected, in triplicate, with the indicated amounts of DNA using Fugene6 transfection reagent (Roche Diagnostics Co.). Forty-eight hours after transfection, luciferase assays were done as described previously (23).

Matrigel assay. Matrigel was diluted to a concentration of 6.3 mg/mL with serum free medium (DMEM) and stored at −80°C. Before use, diluted Matrigel was thawed on ice overnight. For the bottom layer, 200 μL of Matrigel solution was added into a 24-well tissue culture plate and incubated at 37°C for 30 min to allow the Matrigel to solidify. A single cell suspension (5×10^3 cells/10 μL) was then mixed with 190 μL of Matrigel at 4°C and added to the solidified bottom layer. The plates were incubated at 37°C for 30 min to allow the Matrigel to solidify, and 500 μL complete medium containing the appropriated concentration of EGCG or DMSO was then added. Following incubation at 37°C for 5 to 7 days, the cell growth was analyzed using a Zeiss Axiovert 200 M microscope.

Migration and invasion assays. Suspensions of 5×10^5 cells were layered in the upper compartment of a Transwell (Costar) on an 8-mm-diameter polycarbonate filter (8 μm pore size) and incubated at 37°C for the indicated times. For invasion assays, filters were precoated with 30 μg of Matrigel. Migration of the cells to the lower side of the filter was evaluated with the acid phosphatase enzymatic assay using *p*-nitrophenyl phosphate and $OD_{410\ nm}$ determination.

Immunoblot analysis. Cells were rinsed with cold PBS and harvested in lysis buffer [50 mmol/L Tris-HCl (pH 8.0), 5 mmol/L EDTA (pH 8.0), 150 mmol/L NaCl, 0.5 mmol/L DTT, 2 μg/mL aprotinin, 2 μg/mL LP, 0.5 mmol/L phenylmethylsulfonyl fluoride, 0.5% NP40]. Whole cell extracts were obtained by sonication, followed by centrifugation at 14,000 rpm for 30 min. Samples were subjected to electrophoresis in an 8% or 10% polyacrylamide-SDS gel and immunoblotting, as previously described (13). Antibodies against ERα and vimentin were purchased from NeoMarker. Antibodies against Snail (sc-10432) were purchased from Santa Cruz Biotechnology. The E-cadherin and γ-catenin antibodies were purchased from BD Transduction Lab, and the β-actin (AC-15) and FOXO3a antibodies were from Sigma and Upstate Biotechnology, respectively.

RNA preparation and reverse transcription-PCR analysis. Cultures were washed twice with PBS, and total RNA was harvested using the UltraspecII RNA isolation kit (Biotecx), following the manufacturer's instructions. The primers and annealing temperatures used for PCR are as follows: *E-cadherin* 5′-CAGCGTCAACTGGACCATTG-3′ and 5′-CCACCGTTCTCCTCCGTAGA-3′ at 65°C; *MTA3* 5′-CAACCCAGCCTTCA-CATGAGT-3′ and 5′-TTCCACGGGAGAAAGTCCTG-3′ at 65°C and glyceraldehyde-3-phosphate dehydrogenase (*Gapdh*) 5′-TCACCATCTTCCAGGAG-3′ and 5′-GCTTCACCACCTTCTTG-3′ at 60°C. The cycle numbers for each gene and RNA preparation from different cell types were determined to be in the linear and quantitative range in pilot experiments. PCR products were analyzed on 5% acrylamide gels run with 0.5× Tris-borate EDTA buffer and stained with GelStar nucleic acid stain (Bio Whittaker Molecular Applications).

Retroviral gene delivery. The cDNAs of human WT FOXO3a and the A3 mutant and dominant negative FOXO3a (FOXO DN) were excised from the pECE expression vector by *Hin*dIII and *Xba*I digestion and end-filled by Klenow enzyme. The blunt-end fragment was then ligated into the *Sna*BI site of the pBabe-puro ecotropic retroviral vector (29), yielding pBabe-puro-A3FOXO3a and pBabe-puro-dnFOXO3a, respectively. Phoenix packaging cells were used for the generation of retrovirus, which were selected with 500 μg/mL hygromycin to increase Gag and Pol viral protein expression. Briefly, P100 dishes of 80% confluent Phoenix cells were transfected with 15 μg of pBabe-puro-FOXO3a (A3 or DN) or pBabe-puro along with 5 μg of an Env-expressing vector. After 24 h, the medium was changed, and cells were incubated for another 24 h at 32°C to increase retrovirus half-life. Supernatants containing retrovirus were then harvested, filtered, and transferred onto target cells in the presence of 2 μg/mL polybrene (Sigma). After 24 h, infected cells were washed, selected with complete medium plus 4 μg/mL puromycin for 4 days, and expanded in medium containing 1 μg/mL puromycin. As a positive control, cells were infected with the pBabe-puro-GFP retrovirus, indicating more than 90% efficiency in retroviral infection (data not shown).

Downloaded from http://aacrjournals.org/cancerres/article-pdf/67/12/5763/2569018/5763.pdf by guest on 04 May 2023

Results

Green tea polyphenol EGCG promotes a less invasive profile of gene expression in Her-2/neu–overexpressing cells. To further elucidate the molecular mechanisms whereby EGCG alters Her-2/neu–mediated transformation, microarray analysis was done with samples from two independent experiments (Affymetrix Mouse 430A 2.0 chips). RNA samples from NF639 cells treated for 24 h with 60 μg/mL EGCG showed an up-regulation of E-cadherin, α-catenin, ERα, and MTA3 and a down-regulation of the proinvasive master regulators Snail1 and Snail3 compared with control DMSO-treated cells; whereas no differences were seen in the expression of control housekeeping genes β-actin, glyceraldehyde 3-phosphate, peptidylprolyl isomerase A, or phosphoglycerate kinase 1 (data not shown). To verify the findings with microarray, NF639 cells were treated with EGCG or DMSO and total RNA harvested and subjected to analysis for expression of *E-cadherin* and *MTA3* by reverse transcription-PCR (RT-PCR). EGCG treatment induced the expression of these two anti-invasive genes (Fig. 1*A*). Furthermore, when protein extracts were probed for the expression of E-cadherin, a substantial induction was observed (Fig. 1*B*). Similarly, the epithelial marker γ-catenin was induced, whereas expression of Snail was decreased. EGCG treatment also induced expression of FOXO3a and its target gene *ERα* (Fig. 1*B*), consistent with our previous findings (21). Thus, EGCG induces an anti-invasive gene expression signature in the highly malignant Her-2/neu–overexpressing NF639 breast cancer cells.

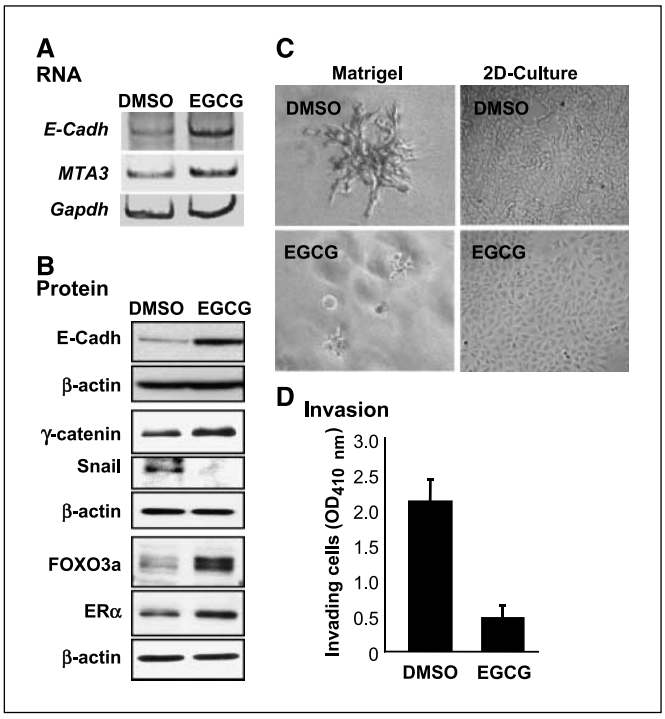

Figure 1. EGCG induces expression of E-cadherin and a more epithelial phenotype. *A* and *B,* NF639 cells were treated with 40 μg/mL EGCG or carrier DMSO for 48 h, and RNA and whole cell protein extracts were prepared. *A*, RNA was subjected to RT-PCR for *E-cadherin* (*E-cadh*), *MTA-3* and *Gapdh*, which confirmed equal loading. *B,* samples of whole cell protein extracts were subjected to immunoblotting for E-cadherin, γ-catenin, Snail, ERα, FOXO3a, and β-actin, which confirmed equal loading. *C, left,* NF639 cells were grown in Matrigel with addition of 40 μg/mL EGCG or carrier DMSO for 5 d. The plates were photographed by a Zeiss Axiovert 200M microscope using an Orca ER camera at 50× magnification (*Matrigel*). *C, right,* NF639 were plated at low confluence in P100 plates and then treated with 40 μg/mL EGCG or carrier DMSO. After 4 d, the cells were photographed at a magnification of 50× (*2D-Culture*). *D,* NF639 cells were treated with 40 μg/mL EGCG or carrier DMSO for 24 h, and then 5×10^5 cells were subjected to an invasion assay for 16 h. $OD_{410\ nm}$ values correspond to cells that migrated to the lower side of the filter and represent the mean of three determinations.

EGCG inhibits invasive phenotype of NF639 cells. One of the hallmarks of invasive mesenchymal phenotype is the branching colony formation in Matrigel. The Her-2/neu–overexpressing NF639 cells, which grow effectively in soft agar (14), formed branched colony structures with a highly invasive phenotype in Matrigel (Fig. 1*C*, DMSO and data not shown). When 40 μg/mL of EGCG was added to the NF639 cells in Matrigel, the branched structures were dramatically reduced (Fig. 1*C, left*). Similar data were obtained upon treatment with 20 μg/mL EGCG (data not shown), which has little effect on growth of these cells (14). Furthermore, the cells took on a more flattened, normal morphology when grown on plastic (Fig. 1*C, right*). Lastly, incubation with EGCG profoundly reduced the ability of NF639 cells to invade through Matrigel (Fig. 1*D*). Together, these data indicate EGCG can reverse the mesenchymal characteristics of Her-2–driven mammary cancer cells, promoting a less invasive phenotype.

EGCG inhibits invasive phenotype of c-Rel– and CK2-driven mammary cancer cells. Almost 90% of human breast cancers contain active, nuclear c-Rel (30), which can play a causal role in mammary tumorigenesis (23). The serine/threonine protein kinase CK2, which has been implicated in basal NF-κB activity (31), is overexpressed in most human breast cancers (32). We next tested the effectiveness of EGCG on invasive tumor lines rel-3875 and rel/CK2-5839 cells, which were derived from mammary tumors in MMTV–c-*rel* transgenic, and MMTV–c-*rel* × MMTV-CK2α bitransgenic mice, respectively. EGCG inhibited the ability of rel-3875 and rel/CK2-5839 cells to form invasive colonies in Matrigel (Fig. 2*A, top*) and induced a more normal, i.e., less elongated, epithelial cell morphology (Fig. 2*A, bottom*). Similarly, invasive colony formation of rel/CK2-5839 cells in Matrigel was inhibited upon treatment with 20 μg/mL EGCG for 1 day, which has no effect on growth rate (data not shown). The effects of EGCG treatment on expression of EMT genes were examined next. Consistent with the morphologic changes, EGCG treatment very effectively induced expression of epithelial markers E-cadherin and γ-catenin and reduced the level of Snail, the repressor of E-cadherin gene transcription, in rel-3875 and rel/CK2-5839 cells (Fig. 2*B*). Furthermore, EGCG treatment led to increased levels of ERα in both lines (Fig. 2*B*). EGCG also profoundly inhibited the ability of rel-3875 cells to invade through Matrigel (Fig. 2*C*), as seen above with NF639 cells. Lastly, we assessed the ability of EGCG to reverse the formation of invasive colonies by rel-3875 cells. After an initial 4 days in Matrigel, substantial invasive colony formation was noted (Fig. 2*D*, day 0). At this time, either EGCG or carrier DMSO was added, and the plates were incubated for an additional 10 days. EGCG completely reverted invasive colony formation, whereas continued growth of invasive colonies was observed in the presence of carrier DMSO (Fig. 2*D*, day 10). Thus, EGCG potently inhibits the invasive properties of breast cancer cells driven by c-*rel* and c-*rel*xCK2, reverting mesenchymal and promoting a more epithelial phenotype.

EGCG induces FOXO3a, which reverses invasive phenotype. Given the pivotal role of ERα in EMT and our findings that FOXO3a is a major regulator of *ERα* gene transcription (21), we next examined the effects of EGCG treatment on FOXO3a expression in rel-3875 and rel/CK2-5839 cells. EGCG caused a substantial

Downloaded from http://aacrjournals.org/cancerres/article-pdf/67/12/5763/2569018/5763.pdf by guest on 04 May 2023

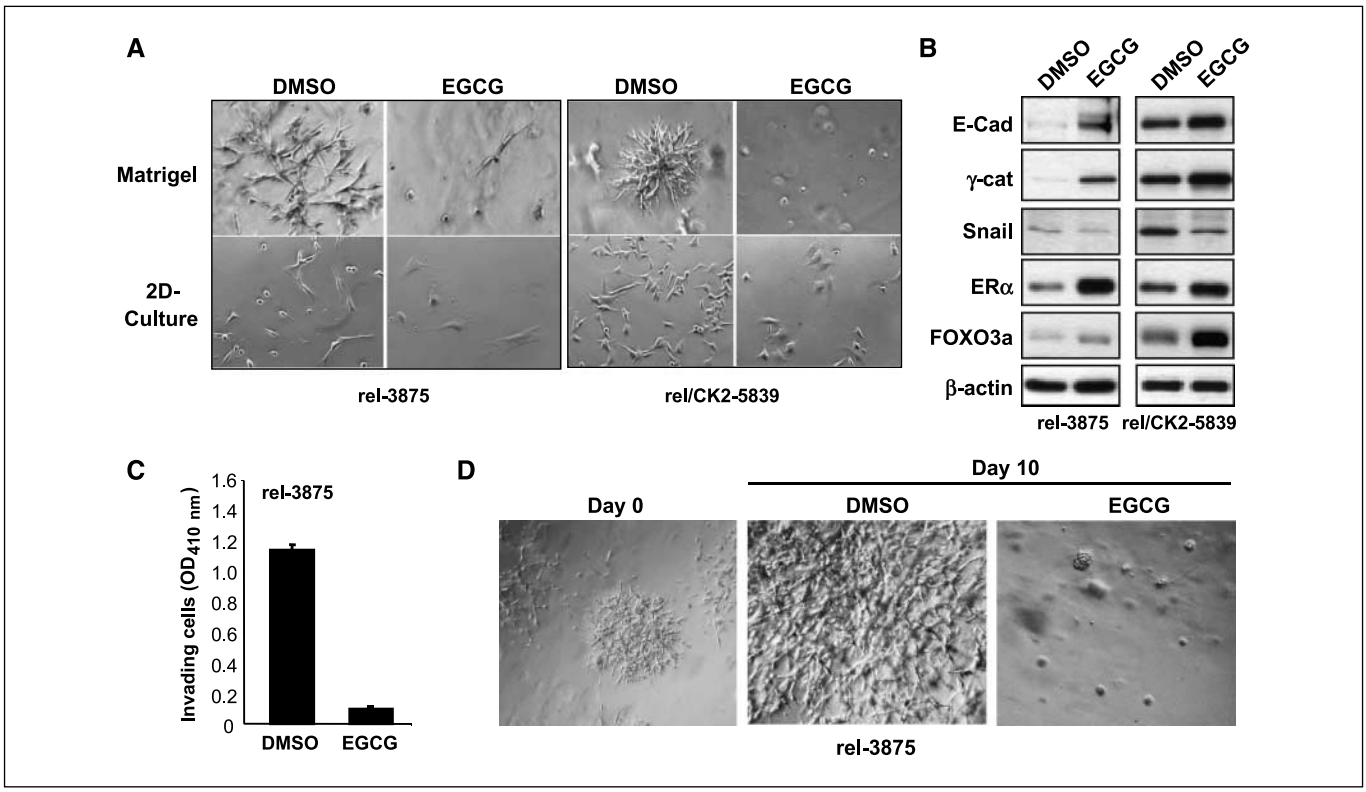

Figure 2. EGCG inhibits invasive phenotype of rel-3875 and rel/CK2-5839 cells. *A, top,* rel-3875 and rel/CK2-5839 cells were grown in Matrigel with addition of 60 μg/mL EGCG or carrier DMSO as control. After 5 d, the colonies were photographed, as above, at a magnification of 50× (*Matrigel*). *A, bottom,* rel-3875 and rel/CK2-5839 cells were plated at low confluence in P100 plates and then treated with 60 μg/mL EGCG or carrier DMSO. After 3 d, the cells were photographed at a magnification of 50× (*2D-Culture*). *B,* rel-3875 and rel/CK2-5839 cells were treated with 60 μg/mL EGCG or carrier DMSO for 72 h, and whole cell protein extracts (25 μg) were subjected to immunoblotting for E-cadherin (*E-Cad*), γ-catenin (*γ-cat*), Snail, ERα, FOXO3a, and β-actin. *C,* rel-3875 cells were treated with 40 μg/mL EGCG or carrier DMSO for 24 h, and then 5×10^5 cells were subjected to an invasion assay for 16 h. $OD_{410\ nm}$ values correspond to cells that migrated to the lower side of the filter and represent the mean of three determinations. *D,* rel-3875 cells were grown in Matrigel, and after 4 d, the colonies were photographed at a magnification of 50× (*Day 0*). At this time, the colonies growing in Matrigel were treated with 40 μg/mL EGCG or carrier DMSO, and after 10 d, the colonies were photographed at a magnification of 50× (*Day 10*).

increase in FOXO3a in the two lines (Fig. 2*B*). To directly test the role of FOXO3a in preventing invasive growth in Matrigel, NF639 cells were infected with either a retrovirus expressing a constitutively active form of FOXO3a (A3; ref. 26) or the empty pBabe vector. The exogenous expression of FOXO3a was confirmed by immunoblotting and led to an induction of E-cadherin protein levels (Fig. 3*A*). Moreover, active FOXO3a reduced the level of Snail protein, the transcriptional repressor of the *E-cadherin* gene (Fig. 3*A*). When plated in Matrigel, the presence of pBabe had minimal effects on the cellular phenotype as judged by the extensive branched structures (Fig. 3*B, top*). Importantly, when A3 FOXO3a-expressing NF639 cells were grown in Matrigel, the branching growth was completely blocked, resulting in the appearance of tightly clustered cells. When grown on plastic, A3 FOXO3a expression caused the cells to have a more epithelial morphology (Fig. 3*B, bottom*), but the growth of the cells was only modestly affected, suggesting that the reduced size of colonies in Matrigel was not simply a result of inhibition of cell cycle progression. Furthermore, ectopic A3 FOXO3a expression caused a substantial decrease in migration of NF639 cells (Fig. 3*C*). These findings could be further extended to the rel/CK2-5839 (Fig. 3*D*), consistent with the observed decrease in levels of the master regulator of EMT Snail (Fig. 3*D, inset*). Thus, sustained FOXO3a activity resulting from the A3 constitutively active mutant reverts the invasiveness conferred by the oncogenic inducers Her-2/neu and c-Rel/CK2.

FOXO3a prevents TGF-β1–induced EMT of NMuMG cells. Another commonly used cell model to study induction of invasive phenotype is the mouse mammary epithelial NMuMG cells, which form a monolayer under normal growth conditions, but change to a fibroblastic phenotype when treated with TGF-β1 (33). This model was used to further assess the role of FOXO3a in EMT. NMuMG cells, infected with a retrovirus expressing either WT FOXO3a, A3 FOXO3a, or the empty pBabe vector, were treated with 1 ng/mL TGF-β1 for 48 h. The expression of the exogenous FOXO3a was confirmed by probing the whole cell extracts with a FOXO3a antibody (Fig. 4*A*). The expression of pBabe, WT, or A3 FOXO3a had minimal effects on the appearance of the cells in the absence of TGF-β1 (Fig. 4*B, left*), although an ~20% reduction of growth rate was observed with cells expressing A3 FOXO3a (data not shown). However, when the cells were grown in the presence of TGF-β1, the pBabe-expressing NMuMG cells appeared spindle shaped, a hallmark of mesenchymal phenotype (Fig. 4*B, right*). Expression of WT FOXO3a resulted in an increased number of flattened cells, indicative of an epithelial phenotype; whereas almost all the cells expressing A3 FOXO3a appeared flattened and epithelial in morphology (Fig. 4*B, right*). The higher potency of A3 FOXO3a in improving the epithelial appearance is consistent with the inability of this FOXO3a mutant to be phosphorylated and thereby inactivated. In particular, treatment of NMuMG cells with TGF-β1 for 48 h resulted in an increase in inactive (phosphorylated) WT

Downloaded from http://aacrjournals.org/cancerres/article-pdf/67/12/5763/2569018/5763.pdf by guest on 04 May 2023

FOXO3a (data not shown). Given the ability of A3 FOXO3a to promote a more epithelial phenotype, we assessed its effects on E-cadherin expression. TGF-β1 treatment resulted in a decrease in E-cadherin levels in the pBabe cells (Fig. 4*C*), consistent with the altered cellular morphology (Fig. 4*B*). In contrast, E-cadherin expression was higher in cells expressing A3 FOXO3a, and the levels were maintained following TGF-β1 treatment (Fig. 4*C*). Hence, functional FOXO3a reduces TGF-β1–mediated EMT of NMuMG cells.

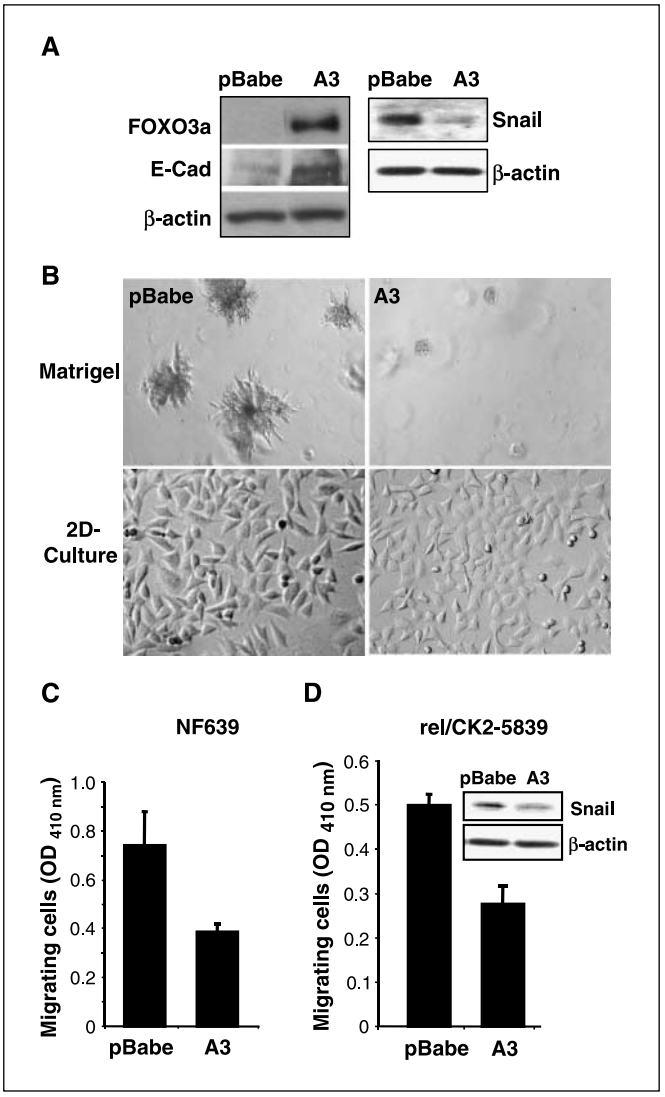

Figure 3. FOXO3a inhibits invasive phenotype of NF639 and rel/CK2-5839 cells. *A,* NF639 cells were infected with a retrovirus control (*pBabe*) or retrovirus expressing A3 FOXO3a (*A3*). Whole cell protein extracts were subjected to immunoblotting for FOXO3a, E-cadherin (*E-cad*), Snail, and β-actin, which showed equal protein loading. *B*, NF639 cells were infected with a retrovirus control (*pBabe*) or retrovirus expressing A3 FOXO3a and grown either in Matrigel or on plastic. *Top,* after 6 d, the colonies in Matrigel were photographed at a magnification of 50×. Representative fields are shown. *Bottom,* NF639 cells infected with control pBabe or pBabe expressing A3 FOXO3a were seeded at a density of 20,000 cells per well in 24-well cell culture dishes. After 3 d, both cultures reached confluence. *C,* NF639 cells were infected with pBabe-puro-A3 FOXO3a (*A3*) or pBabe-puro (*pBabe*) retrovirus. After 7 d of selection with puromycin, 5×10^5 cells were subjected to a migration assay for 6 h. $OD_{410\ nm}$ values correspond to cells that migrated to the lower side of the filter and represent the mean of three determinations. *D,* rel/CK2-5839 cells were infected with pBabe-puro-A3 FOXO3a or pBabe-puro retrovirus. After 7 d of selection with puromycin, 5×10^5 cells were subjected to a migration assay for 6 h. $OD_{410\ nm}$ values correspond to cells that migrated to the lower side of the filter and represent the mean of three determinations. *Inset,* whole cell protein extracts prepared from rel/CK2-5839 cells infected with control pBabe or pBabe expressing A3 FOXO3a were subjected to immunoblotting for Snail and β-actin.

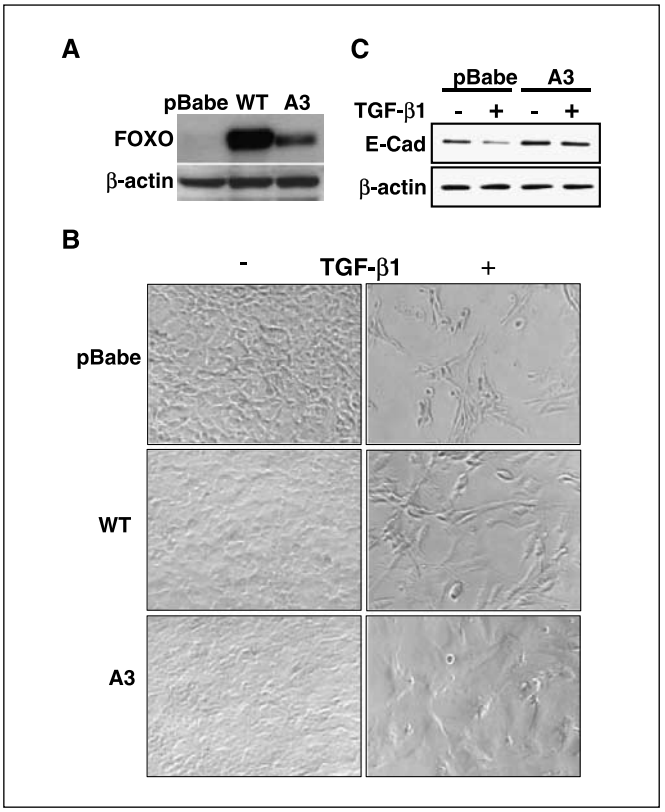

Figure 4. FOXO3A prevents TGF-β1–induced EMT in NMuMG cells. *A* and *B,* NMuMG cells were infected with either the pBabe-puro (pBabe), pBabe-puro-WT FOXO3a (*WT*) or pBabe-puro-A3 FOXO3a (*A3*) retrovirus. After 4 d of selection with puromycin, whole cell protein extracts were prepared from the indicated cells and subjected to immunoblotting for FOXO3a (*FOXO*) and β-actin (*A*). Alternatively, cells were plated and then treated with 1 ng/mL TGF-β1 (+) or its control solution 0.1% bovine serum albumin (BSA) in 4 mmol/L HCl (−). After 10 d, the cells were photographed at a magnification of 50× (*B*). *C,* NMuMG cells were infected with pBabe-puro-A3 FOXO3a or pBabe-puro retrovirus. After 5 d of selection with puromycin, cells were plated at low confluence and treated with 1 ng/mL TGF-β1 (+) or its control solution 0.1% BSA in 4 mmol/L HCl (−) for 48 h. Whole cell protein extracts (10 μg) were subjected to immunoblotting for E-cadherin and β-actin.

FOXO3a induces E-cadherin expression via ERα signaling. We next hypothesized that ectopic expression of FOXO3a in NMuMG cells activates the ERα to E-cadherin pathway. NMuMG cells were transfected with vectors expressing the empty vector pECE, WT, or constitutively active A3 FOXO3a. Whole cell protein extracts were probed for the expression of E-cadherin (Fig. 5*A*). Expression of both WT and A3 FOXO3a induced E-cadherin protein levels, with the constitutively active A3 FOXO3a again being more effective, consistent with our previous findings, demonstrating that it more effectively induces ERα promoter activity and expression than WT FOXO3a (21). Immunoblotting confirmed ectopic expression of WT, and A3 FOXO3a was essentially equivalent, and Coomassie blue staining of proteins showed equal loading (Fig. 5*A*). In agreement with the increase in protein levels, RT-PCR showed both WT and A3 FOXO3a increased *E-cadherin* mRNA levels in transfected cells, with the A3 FOXO3a again leading to a

Downloaded from http://aacrjournals.org/cancerres/article-pdf/67/12/5763/2569018/5763.pdf by guest on 04 May 2023

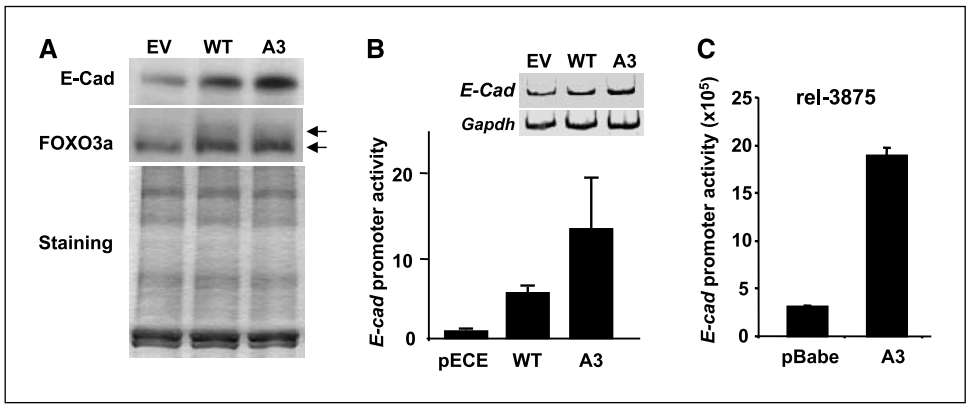

Figure 5. FOXO3a induces E-cadherin expression. *A,* NMuMG cells were transfected with empty vector pECE (*EV*), WT, or A3 FOXO3a. Approximately 40 h after transfection, cells were harvested, and whole cell protein extracts were prepared for immunoblotting for E-cadherin and FOXO3a. Coomassie blue staining (*Staining*) of the blot was used as a loading control because β-actin was run off the gel to achieve the separation of different phospho-FOXO3a species. *B,* NMuMG cells were transiently transfected, in triplicate, in six-well plates with 0.5 μg E-cadherin promoter-Luc vector, 0.5 μg SV40-β-gal and 1 μg empty vector pECE, WT, or A3 FOXO3a. Forty-eight hours after transfection, luciferase activity was measured and normalized to β-gal activity. *Inset,* NMuMG cells were transfected with pECE (*EV*), WT, and A3 FOXO3a. Approximately 40 h after transfection, total RNA was prepared, and the mRNA expression of *E-cadherin* (*E-Cad*) and *Gapdh* was assessed by RT-PCR analysis. *C,* rel-3875 cells were transiently transfected, in triplicate, in 12-well plates with 0.1 μg *E-cadherin* (*E-cad*) promoter-Luc vector, 0.1 μg SV40-β-gal, and 0.3 μg pBabe-puro-A3FOXO3a or pBabe-puro. Forty-eight hours after transfection, luciferase activity was measured and normalized to β-gal activity.

more substantial effect (Fig. 5*B, inset*). Next, we tested the ability of the A3 FOXO3a protein to induce *E-cadherin* promoter activity. Expression of the A3 FOXO3a led to a potent activation of the *E-cadherin* promoter in both NMuMG (Fig. 5*B*) and rel-3875 cells (Fig. 5*C*).

We next asked whether a dominant negative FOXO3a (FOXO DN) can induce mesenchymal gene expression. Untransformed NMuMG cells were infected with either pBabe or FOXO DN, and whole cell extracts were analyzed. The dominant negative FOXO3a reduced E-cadherin and γ-catenin levels and increased the expression of Snail (Fig. 6*A*). Expression of the dominant negative FOXO3a similarly repressed E-cadherin protein level in rel-3875 and rel/CK2-5839 cells (Fig. 6*B*). Expression of ERα, a known target of FOXO3a, was potently reduced by expression of the dominant negative FOXO3a, confirming the efficiency of this mutant to block FOXO3a activity (Fig. 6*B*). Thus, FOXO3a induces a gene expression profile associated with a more epithelial phenotype in rel-3875 and rel/CK2-5839 cells, which express low level of ERα, similar to NF639 cells (ref. 21 and data not shown).

To test the role of ERα in FOXO3a signaling to E-cadherin expression, two approaches were used. We first subjected the prototypical ERα-negative MDA-MB-231 cancer cell line to similar analysis. A3 FOXO3a failed to induce E-cadherin expression in MDA-MB-231 cells (Fig. 6*C*). Immunoblotting confirmed FOXO3a expression. We next tested whether inhibition of ERα blocks the effects of FOXO3a on EMT in ERα-positive rel/CK2-5839 cells.

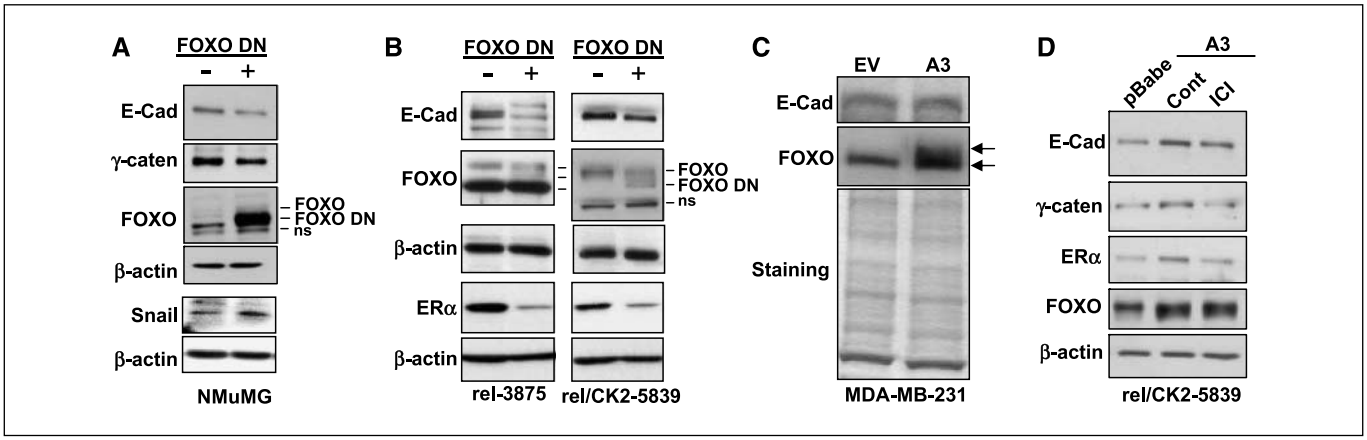

Figure 6. FOXO3a induces a more epithelial gene expression profile in ERα-low breast cancer cells. *A,* NMuMG cells were infected with pBabe-puro-dnFOXO3a (*FOXO DN*) or pBabe-puro (−) retrovirus and selected for 4 d with puromycin. Whole cell protein extracts (15 μg) were subjected to immunoblotting for E-cadherin (*E-cad*), γ-catenin (*γ-caten*), FOXO3a (*FOXO*), Snail, and β-actin. Positions of FOXO3a, FOXO3a DN, and non-specific bands (*ns*) are as indicated. *B,* rel-3875 and rel/CK2-5839 cells, respectively, were transfected or infected with pBabe-puro-dnFOXO3a (*FOXO DN*) or pBabe-puro (−) retrovirus and selected for 4 d with puromycin. Whole cell protein extracts (50 μg for rel-3875 cells and 20 μg for rel/CK2-5839 cells) were subjected to immunoblotting for E-cadherin, FOXO3a, ERα, and β-actin. Positions of FOXO3a, FOXO3a DN, and nonspecific bands are as indicated. *C,* MDA-MB-231 cells were transfected with parental pECE (*EV*) or A3 FOXO3a (*A3*) DNA. Approximately 40 h after transfection, whole cell protein extracts were prepared and subjected to immunoblotting for E-cadherin and FOXO3a. Coomassie blue staining of the blot was used to control for equal loading because the gel was electrophoresed extensively to achieve better separation of hypo- and hyperphosphorylated FOXO3a species, such that β-actin was run off the gel. *D,* rel/CK2-5839 cells were infected with pBabe-puro-A3 FOXO3a (*A3*) or pBabe-puro (*pBabe*) retrovirus. After 4 d of selection with puromycin, cells were plated and then treated with 1 μmol/L ICI 182,780 (*ICI*) or vehicle ethanol (*Cont*) for 48 h. Whole cell protein extracts (20 μg) were subjected to immunoblotting for E-cadherin, γ-catenin, ERα, FOXO3a, and β-actin.

Downloaded from http://aacrjournals.org/cancerres/article-pdf/67/12/5763/2569018/5763.pdf by guest on 04 May 2023

Ectopic expression of A3 FOXO3a induced the levels of E-cadherin and γ-catenin, as well as ERα, as expected (Fig. 6*D*). The addition of the antiestrogen ICI 182,780, which inhibits estrogen-dependent ERα function (34) and decreases ERα protein levels (35), blocked the activation of the E-cadherin and γ-catenin genes by FOXO3a (Fig. 6*D*). Taken together, these data indicate that FOXO3a confers anti-invasive properties in breast cancer cells via an ERα-mediated pathway.

Discussion

Here, we show for the first time a role for the Forkhead family member FOXO3a in control of EMT of ERα-low breast cancer cells. Recently, we identified two forkhead elements upstream of ERα promoter B and showed that FOXO3a can potently activate ERα gene transcription (21), which was confirmed by Madureira et al. (36). Activation of FOXO3a and resulting enhanced ERα signaling by EGCG promoted a less malignant phenotype of breast cancer cells. ERα signaling has been shown to promote a more epithelial phenotype via inhibiting synthesis of Snail, a repressor of E-cadherin expression (16). ERα can induce synthesis of MTA3, a component of the HDAC NuRD, which inhibits *Snail* gene transcription. In the presence of active ERα signaling, we noted that EGCG induced a more epithelial gene expression profile, i.e., increased expression of MTA3, E-cadherin, γ-catenin while repressing Snail. Of note, FOXO3a inhibited the formation of invasive colonies in Matrigel, invasive phenotype induced by TGF-β1 signaling, and reduced the ability of cells to migrate. In the absence of ERα signaling, this movement of gene expression toward an epithelial phenotype did not occur. Hence, our studies place FOXO3a upstream of ERα in the MTA3/NuRD pathway that represses the expression Snail and thereby promotes a less invasive, more epithelial phenotype.

The ability of active FOXO3a to functionally promote a less invasive phenotype via ERα signaling defines a novel aspect for FOXO proteins as potential tumor suppressors. FOXO proteins have been shown to induce cell cycle arrest, maintain genome stability, and promote apoptosis largely by inducing *p27, GADD45*, and *BIM* gene expression, respectively (27, 37, 38). In breast cancer patients, inactive cytoplasmic FOXO3a expression correlates with poor survival (39). Inhibition of FOXO3a increases tumorigenesis in nude mice (39). Although the overall antitumor effect of FOXO3a is likely mediated through the combination of mechanisms, our data suggest that FOXO3a contributes through the activation of the ERα/MTA3/E-cadherin pathway. Recently, it was reported that FOXM1, another forkhead protein, interacts with FOXO3a and cooperatively regulates ERα expression (36). It remains to be determined how this interaction affects invasive phenotype.

The mechanism we report here extends the known ability of EGCG to promote a more epithelial phenotype via its antioxidative activity. Tumor cells produce large amounts of reactive oxygen species (ROS), which leads to the induction of matrix metalloproteinases that promote invasion and metastasis (40, 41). The antioxidative activity of green tea polyphenols was found to potently inhibit many matrix proteinases (42–44). ROS scavengers have been seen to inhibit FOXO3a induction (45), suggesting ROS is capable of inducing FOXO3a. The observed activation of FOXO3a by EGCG likely occurs via a mechanism that is independent of its antioxidative activity. Interestingly, FOXO proteins have been shown to protect from oxidative damage–induced apoptosis by inducing the antioxidant enzymes MnSOD and catalase (46). Whether induction of MnSOD by FOXO3a contributes to the inhibition of an invasive phenotype remains to be determined.

In summary, our study offers a novel molecular understanding of the observed anticarcinogenic effect of green tea. EGCG possesses potent anti-invasive activity by activating the FOXO3a/ERα/MTA3/E-cadherin pathway. Substantial anticarcinogenic effects have been seen in studies in animal drinking doses comparable to 3 to 10 cups daily (reviewed in ref. 1). Green tea extracts potently reduce (87%) invasive phenotype of mammary tumors induced by DMBA in S-D rats (5). Oral infusion of a polyphenolic fraction isolated from green tea significantly inhibited prostate cancer development and increased survival of TRAMP mice (6). A study in Japan has found that drinking green tea, at the level used in these animal studies, reduced the risk of recurrence in women with stage I and II breast cancer (3). Thus, green tea and EGCG offer attractive antitumorigenic agents that can be easily and safely incorporated into daily lives.

Acknowledgments

Received 11/28/2006; revised 4/9/2007; accepted 4/17/2007.

Grant support: NIH PO1 ES11624 and a grant from the Avon Foundation.

The costs of publication of this article were defrayed in part by the payment of page charges. This article must therefore be hereby marked *advertisement* in accordance with 18 U.S.C. Section 1734 solely to indicate this fact.

We thank M. Greenberg and A. Brunet for providing cloned FOXO DNAs, P. Leder for the NF639 cell line, C. Taylor for assistance with the microarray analysis, and K. Kirsch for generously allowing access to the microscope and camera. We also thank Junfeng Wu for preparing the E-cad-Luc construct.

Downloaded from http://aacrjournals.org/cancerres/article-pdf/67/12/5763/2569018/5763.pdf by guest on 04 May 2023

References

1. Guo S, Sonenshein GE. Mechanisms of green tea action. In: Kaput J, Rodriguez R, editors. Nutritional genomics: discovering the path to personalized nutrition. Wiley and Sons; 2006, p. 177–206.
2. Nakachi K, Suemasu K, Suga K, Takeo T, Imai K, Higashi Y. Influence of drinking green tea on breast cancer malignancy among Japanese patients. Jpn J Cancer Res 1998;89:254–61.
3. Inoue M, Tajima K, Mizutani M, et al. Regular consumption of green tea and the risk of breast cancer recurrence: follow-up study from the Hospital-based Epidemiologic Research Program at Aichi Cancer Center (HERPACC), Japan. Cancer Lett 2001;167:175–82.
4. Hirose M, Hoshiya T, Akagi K, Futakuchi M, Ito N. Inhibition of mammary gland carcinogenesis by green tea catechins and other naturally occurring antioxidants in female Sprague-Dawley rats pretreated with 7,12-dimethylbenz[α]anthracene. Cancer Lett 1994;83:149–56.
5. Kavanagh KT, Hafer LJ, Kim DW, et al. Green tea extracts decrease carcinogen-induced mammary tumor burden in rats and rate of breast cancer cell proliferation in culture. J Cell Biochem 2001;82:387–98.
6. Gupta S, Hastak K, Ahmad N, Lewin JS, Mukhtar H. Inhibition of prostate carcinogenesis in TRAMP mice by oral infusion of green tea polyphenols. Proc Natl Acad Sci U S A 2001;98:10350–5.
7. Conney AH, Wang ZY, Huang MT, Ho CT, Yang CS. Inhibitory effect of green tea on tumorigenesis by chemicals and ultraviolet light. Prev Med 1992;21:361–9.
8. Ignatoski KM, Maehama T, Markwart SM, Dixon JE, Livant DL, Ethier SP. ERBB-2 overexpression confers PI 3′ kinase-dependent invasion capacity on human mammary epithelial cells. Br J Cancer 2000;82:666–74.
9. Tokatli F, Altaner S, Uzal C, et al. Association of HER-2/neu overexpression with the number of involved axillary lymph nodes in hormone receptor positive breast cancer patients. Exp Oncol 2005;27:145–9.
10. Astolfi A, Landuzzi L, Nicoletti G, et al. Gene expression analysis of immune-mediated arrest of tumorigenesis in a transgenic mouse model of HER-2/neu-positive basal-like mammary carcinoma. Am J Pathol 2005;166:1205–16.
11. Madrid LV, Wang CY, Guttridge DC, Schottelius AJ, Baldwin AS, Jr., Mayo MW. Akt suppresses apoptosis by stimulating the transactivation potential of the RelA/p65 subunit of NF-κB. Mol Cell Biol 2000;20:1626–38.
12. Sizemore N, Leung S, Stark GR. Activation of phosphatidylinositol 3-kinase in response to interleukin-1 leads to phosphorylation and activation of the NF-κB p65/RelA subunit. Mol Cell Biol 1999;19:4798–805.
13. Pianetti S, Arsura M, Romieu-Mourez R, Coffey RJ, Sonenshein GE. Her-2/neu overexpression induces

NF-κB via a PI3-kinase/Akt pathway involving calpain-mediated degradation of IκB-α that can be inhibited by the tumor suppressor PTEN. Oncogene 2001;20:1287–99.
14. Pianetti S, Guo S, Kavanagh KT, Sonenshein GE. Green tea polyphenol epigallocatechin-3 gallate inhibits Her-2/neu signaling, proliferation, and transformed phenotype of breast cancer cells. Cancer Res 2002;62:652–5.
15. Garcia M, Derocq D, Freiss G, Rochefort H. Activation of estrogen receptor transfected into a receptor-negative breast cancer cell line decreases the metastatic and invasive potential of the cells. Proc Natl Acad Sci U S A 1992;89:11538–42.
16. Fujita N, Jaye DL, Kajita M, Geigerman C, Moreno CS, Wade PA. MTA3, a Mi-2/NuRD complex subunit, regulates an invasive growth pathway in breast cancer. Cell 2003;113:207–19.
17. Kang Y, Massague J. Epithelial-mesenchymal transitions: twist in development and metastasis. Cell 2004;118:277–9.
18. Bachelder RE, Yoon SO, Franci C, de Herreros AG, Mercurio AM. Glycogen synthase kinase-3 is an endogenous inhibitor of Snail transcription: implications for the epithelial-mesenchymal transition. J Cell Biol 2005;168:29–33.
19. Konecny G, Pauletti G, Pegram M, et al. Quantitative association between HER-2/neu and steroid hormone receptors in hormone receptor-positive primary breast cancer. J Natl Cancer Inst 2003;95:142–53.
20. Moe RE, Moe KS, Porter P, Gown AM, Ellis G, Tapper D. Expression of Her-2/neu oncogene protein product and epidermal growth factor receptors in surgical specimens of human breast cancers. Am J Surg 1991;161:580–3.
21. Guo S, Sonenshein GE. Forkhead box transcription factor FOXO3a regulates estrogen receptor α expression and is repressed by the Her-2/neu/phosphatidylinositol 3-kinase/Akt signaling pathway. Mol Cell Biol 2004;24:8681–90.
22. Elson A, Leder P. Protein-tyrosine phosphatase epsilon. An isoform specifically expressed in mouse mammary tumors initiated by v-Ha-ras OR neu. J Biol Chem 1995;270:26116–22.
23. Romieu-Mourez R, Kim DW, Shin SM, et al. Mouse mammary tumor virus c-rel transgenic mice develop mammary tumors. Mol Cell Biol 2003;23:5738–54.
24. Eddy SF, Guo S, Demicco EG, et al. Inducible IκB kinase/IκB kinase epsilon expression is induced by CK2 and promotes aberrant nuclear factor-κB activation in breast cancer cells. Cancer Res 2005;65:11375–83.
25. Song DH, Sussman DJ, Seldin DC. Endogenous protein kinase CK2 participates in Wnt signaling in mammary epithelial cells. J Biol Chem 2000;275:23790–7.
26. Brunet A, Bonni A, Zigmond MJ, et al. Akt promotes cell survival by phosphorylating and inhibiting a Forkhead transcription factor. Cell 1999;96:857–68.
27. Tran H, Brunet A, Grenier JM, et al. DNA repair pathway stimulated by the forkhead transcription factor FOXO3a through the Gadd45 protein. Science 2002;296:530–4.
28. Batsche E, Muchardt C, Behrens J, Hurst HC, Cremisi C. RB and c-Myc activate expression of the E-cadherin gene in epithelial cells through interaction with transcription factor AP-2. Mol Cell Biol 1998;18:3647–58.
29. Morgenstern JP, Land H. Advanced mammalian gene transfer: high titre retroviral vectors with multiple drug selection markers and a complementary helper-free packaging cell line. Nucleic Acids Res 1990;18:3587–96.
30. Sovak MA, Bellas RE, Kim DW, et al. Aberrant nuclear factor-κB/Rel expression and the pathogenesis of breast cancer. J Clin Invest 1997;100:2952–60.
31. Romieu-Mourez R, Landesman-Bollag E, Seldin DC, Sonenshein GE. Protein kinase CK2 promotes aberrant activation of nuclear factor-κB, transformed phenotype, and survival of breast cancer cells. Cancer Res 2002;62:6770–8.
32. Landesman-Bollag E, Romieu-Mourez R, Song DH, Sonenshein GE, Cardiff RD, Seldin DC. Protein kinase CK2 in mammary gland tumorigenesis. Oncogene 2001;20:3247–57.
33. Miettinen PJ, Ebner R, Lopez AR, Derynck R. TGF-β induced transdifferentiation of mammary epithelial cells to mesenchymal cells: involvement of type I receptors. J Cell Biol 1994;127:2021–36.
34. Hyder SM, Chiappetta C, Murthy L, Stancel GM. Selective inhibition of estrogen-regulated gene expression *in vivo* by the pure antiestrogen ICI 182,780. Cancer Res 1997;57:2547–9.
35. Oliveira CA, Nie R, Carnes K, et al. The antiestrogen ICI 182,780 decreases the expression of estrogen receptor-α but has no effect on estrogen receptor-β and androgen receptor in rat efferent ductules. Reprod Biol Endocrinol 2003;1:75–86.
36. Madureira PA, Varshochi R, Constantinidou D, et al. The Forkhead box M1 protein regulates the transcription of the estrogen receptor α in breast cancer cells. J Biol Chem 2006;281:25167–76.
37. Stahl M, Dijkers PF, Kops GJ, et al. The forkhead transcription factor FoxO regulates transcription of p27Kip1 and Bim in response to IL-2. J Immunol 2002;168:5024–31.
38. Medema RH, Kops GJ, Bos JL, Burgering BM. AFX-like Forkhead transcription factors mediate cell-cycle regulation by Ras and PKB through p27kip1. Nature 2000;404:782–7.
39. Hu MC, Lee DF, Xia W, et al. IκB kinase promotes tumorigenesis through inhibition of forkhead FOXO3a. Cell 2004;117:225–37.
40. Brenneisen P, Briviba K, Wlaschek M, Wenk J, Scharffetter-Kochanek K. Hydrogen peroxide (H_2O_2) increases the steady-state mRNA levels of collagenase/MMP-1 in human dermal fibroblasts. Free Radic Biol Med 1997;22:515–24.
41. Nonaka Y, Iwagaki H, Kimura T, Fuchimoto S, Orita K. Effect of reactive oxygen intermediates on the *in vitro* invasive capacity of tumor cells and liver metastasis in mice. Int J Cancer 1993;54:983–6.
42. Sazuka M, Imazawa H, Shoji Y, Mita T, Hara Y, Isemura M. Inhibition of collagenases from mouse lung carcinoma cells by green tea catechins and black tea theaflavins. Biosci Biotechnol Biochem 1997;61:1504–6.
43. Jankun J, Selman SH, Swiercz R, Skrzypczak-Jankun E. Why drinking green tea could prevent cancer. Nature 1997;387:561.
44. Garbisa S, Sartor L, Biggin S, Salvato B, Benelli R, Albini A. Tumor gelatinases and invasion inhibited by the green tea flavanol epigallocatechin-3-gallate. Cancer 2001;91:822–32.
45. Liu JW, Chandra D, Rudd MD, et al. Induction of prosurvival molecules by apoptotic stimuli: involvement of FOXO3a and ROS. Oncogene 2005;24:2020–31.
46. Kops GJ, Dansen TB, Polderman PE, et al. Forkhead transcription factor FOXO3a protects quiescent cells from oxidative stress. Nature 2002;419:316–21.

Downloaded from http://aacrjournals.org/cancerres/article-pdf/67/12/5763/2569018/5763.pdf by guest on 04 May 2023